

## The Photodisintegration of the Deuteron at Intermediate Energies. I.

C. A. BARNES,\* J. H. CARVER, G. H. STAFFORD,† AND D. H. WILKINSON  
*Cavendish Laboratory, University of Cambridge, Cambridge, England*

(Received December 14, 1951)

Measurements have been made of the absolute cross section for photodisintegration of the deuteron at six gamma-ray energies in a range where the photomagnetic effect is small compared with the photoelectric. The methods of determining the gamma-ray flux are described as are the high pressure deuterium-filled ionization chamber and proportional counter used to determine the disintegration rate. The results are given in the following table, together with the reactions used to provide the gamma-rays.

Reaction	Gamma-ray energy (Mev)	Cross section ( $\times 10^{28}$ cm <sup>2</sup> )
$N^{15}(\beta, \alpha)C^{12*}$	$4.45 \pm 0.04$	$24.3 \pm 1.7$
$F^{19}(\beta, \alpha)O^{16*}$	$6.14 \pm 0.01$	$21.9 \pm 1.0$
$Be^9(\beta, \gamma)B^{10}$	$7.39 \pm 0.15$	$18.4 \pm 1.5$
$C^{13}(\beta, \gamma)N^{14}$	$8.14 \pm 0.08$	$18.0 \pm 1.3$
$B^{11}(\beta, \gamma)C^{12*}$	$12.50 \pm 0.21$	$10.4 \pm 1.0$
$Li^7(\beta, \gamma)Be^8$	$17.6 \pm 0.2$	$7.7 \pm 0.9$

### INTRODUCTION

THE photodisintegration of the deuteron gives direct information about the neutron-proton system in the triplet state, for this state constitutes the bulk of the deuteron ground state. The total cross section for photodisintegration by gamma-rays of energy remote from the threshold, say above 4 Mev, is governed largely by the binding energy of the deuteron and by the effective range of the neutron-proton triplet interaction.<sup>1-4</sup> Although the absolute cross section depends on the details of the neutron-proton interaction, the form of the cross section's dependence on gamma-ray energy does not, provided this energy remains below about 20 Mev.<sup>5,6</sup>

Measurements of the cross section for photodisintegration of the deuteron have been made in the range of gamma-ray energy from 4.5 to 17.6 Mev. The first objective of these measurements was to determine the form of the dependence of the cross section on gamma-ray energy. Agreement between this form and that predicted by theory for forces of zero range<sup>7</sup> furnishes a check on the applicability of quantum mechanics to the calculation of transitions between states of the two-nucleon system. The second objective was the determination of the ratio between the cross sections and those predicted by theory for forces of zero range. This ratio then determines the effective range very directly.<sup>3,4</sup> A third objective was the provision of an anchor for high energy photodisintegration experiments where details of the neutron-proton interaction poten-

tial shape, for example, become important.<sup>5,6</sup> This demands the successful attainment of the first objective and the agreement between the effective range as deduced from these measurements and that derived by other means.

This paper describes the experiments; the following paper presents a discussion of the results.

### GENERAL METHOD

Measurements have been made at 4.45, 6.14, 7.39, 8.14, 12.5, and 17.6 Mev. The method for all energies except the first was to irradiate a known mass of deuterium gas contained in an ionization chamber with a known flux of the gamma-rays in question and to determine the disintegration rate by counting the photoprotons. The cross section at 4.45 Mev was found by irradiating a proportional counter containing deuterium with known fluxes of 4.45- and 6.14-Mev gamma-rays. The ratio of the cross sections at the two energies was determined.

### THE IONIZATION CHAMBER

Electrons must remain free in the gas of the ionization chamber. The gas pressure must be high because the cross section to be measured is small, and sufficient stopping power must be provided for the photoprotons to dissipate all their energy in the gas. The purity of the gas must then be very great.<sup>8</sup> The ionization chamber proper was spherical so that the geometrical effects of photoprotons striking the walls could be accurately calculated. The collecting electrode was a thin rod to minimize the inductive effects of positive ions. A steel envelope of thickness 0.67 cm closely surrounded the chamber proper, which was a spherical glass vessel of diameter 9.6 cm. The anode was an aluminum rod of diameter 0.3 cm and was held axially

\* Now at the University of British Columbia, Vancouver, Canada.

† Now at the University of Pretoria, Pretoria, South Africa.

<sup>1</sup> J. M. Blatt and J. D. Jackson, *Phys. Rev.* **76**, 18 (1949).

<sup>2</sup> H. A. Bethe, *Phys. Rev.* **76**, 38 (1949).

<sup>3</sup> H. A. Bethe and C. Longmire, *Phys. Rev.* **77**, 647 (1950).

<sup>4</sup> E. E. Salpeter, *Phys. Rev.* **82**, 60 (1951).

<sup>5</sup> L. I. Schiff, *Phys. Rev.* **78**, 733 (1950).

<sup>6</sup> J. F. Marshall and E. Guth, *Phys. Rev.* **78**, 738 (1950).

<sup>7</sup> H. A. Bethe and R. Peierls, *Proc. Roy. Soc. (London)* **A148**, 146 (1935).

<sup>8</sup> D. H. Wilkinson, *Ionization Chambers and Counters* (Cambridge University Press, London, 1950).

within the sphere. There was no cathode within the glass chamber, but the outside of the vessel was painted with Aquadag, to within 3 cm of the axis; this Aquadag coating was the cathode as in the Geiger counter of Maze.<sup>9</sup> The anode passed into small side-arms on which were painted Aquadag guard-rings. In this way a chamber of well-defined volume was achieved. The chamber was filled with distilled water and weighed; from the volume measured in this way was subtracted the calculated volumes of the side arms. The effective volume was 475 cc. The chamber was baked in an atmosphere of hydrogen for 8 hours at 400°C; it was then baked for a further 8 hours at a pressure of  $10^{-6}$  mm Hg, flushed with pure hydrogen at a pressure of  $10^{-3}$  mm Hg for 1 hour and sealed off. It was then mounted in the steel shell and was filled with pure deuterium by filtering this gas through palladium tubes which were attached to the glass chamber.<sup>10</sup> The pressure in the outer shell was increased at the rate of 1 atmosphere per hour. The pressure finally reached was 38.15 atmospheres (at 0°C). The measurement was made on the gas within the steel shell with a pressure gauge which had been calibrated by the National Physical Laboratory; it was made several weeks after filling to ensure that equilibrium had been reached. The chamber was operated under a potential difference of 10,000 volts: this was furnished by batteries. Under these conditions electron collection appeared to be complete.

#### THE RESOLUTION OF THE IONIZATION CHAMBER

There are three chief reasons why, on irradiation with monochromatic gamma-rays, this chamber does not yield a perfectly sharp group of photoproton pulses. One is that, due to the ballistics of the reaction, there exists a spread of about 20 percent in the photoproton energy. Another reason is the inductive effects of the positive ions; this means that the pulse produced by the liberation of a given amount of ionization depends on the location of that ionization within the chamber. This effect is calculable.<sup>8</sup> Calculations have been made for the present chamber under two approximations. The first approximation replaces the chamber by infinite coaxial cylinders of radii  $b$  and  $a$ , the second by confocal ellipsoids. The results of these two approximations differ only slightly, and the correct result lies between them: we assume that our chamber may be represented by infinite coaxial cylinders with  $b^2/a^2=6000$ . The result of the calculation of the inductive effects between confocal ellipsoids is stated in Appendix I. The ballistic spread and the inductive effect are combined analytically in Appendix II. The resolution of the chamber calculated in this way agreed very well with that experimentally observed and gave confidence that the apparatus was working properly. This calculation may also be used to demonstrate that, despite the fact that

the ballistic spread is a function of gamma-ray energy while the inductive spread is not, the peak in the photoproton pulse distribution may be taken as a direct measure of the mean photoproton energy and so be directly related to the gamma-ray energy.<sup>11,12</sup>

The wall effect also distorts the pulse distribution. Some photoprotons strike the wall before reaching the end of their range and so give a reduced pulse. This effect may be simply calculated for a spherical chamber. The result is stated in Appendix III.

These considerations enable the expected pulse distribution to be computed with some accuracy, and, by comparing this with the experimental pulse distribution, the total disintegration rate may be accurately determined even though the photoproton range may become comparable with the dimensions of the chamber.

We have also considered the effects of collisions between deuterons of the chamber gas and the photoneutrons produced both within the chamber proper and between the glass chamber and the steel outer shell. Both effects are small.

The smearing effect on the calculated distributions of the noise due to the amplifier and to the building up of pulses due to fast electrons must be allowed for.

#### THE FINITE SIZE OF THE IONIZATION CHAMBER

Owing to the finite size of the ionization chamber we may not assume, for the purposes of relating the gamma-ray flux with the observed disintegration rate, that all the gas is concentrated at the center of the sphere. If the gamma-ray source is a disk of diameter small compared with that of the sphere, as it is under our experimental conditions, the departure from the inverse square law may be allowed for by dividing all the disintegration rates by

$$f(x) = \frac{3x^2}{2} \left\{ 1 - \frac{x^2-1}{x} \log \left[ \frac{x+1}{(x^2-1)^{\frac{1}{2}}} \right] \right\},$$

where  $x$  is the distance of the center of the sphere from the gamma-ray source divided by the radius of the sphere.

#### THE PROPORTIONAL COUNTER

The ionization chamber could not be applied directly to the measurements at 4.45 Mev because the pulses resulting from fast electrons became comparable in size with those resulting from photoprotons. A proportional counter was built for work at this energy. The body was a stainless steel cylinder of length 30 cm and diameter 10 cm; the wall thickness was 2 mm. A tungsten wire of diameter  $40\mu$  hung along the axis of the counter and was held taut by a nickel weight. The exposed length

<sup>11</sup> Provided that  $W$ , the energy required to create one ion pair, is a good constant for protons in deuterium. This is very probably so, and extra confidence is given by the fact that  $W$  for protons of 340 Mev in hydrogen is only 3 percent lower than for slow protons (see reference 12).

<sup>12</sup> C. J. Bakker and E. Segrè, Phys. Rev. 81, 489 (1951).

<sup>9</sup> R. Maze, J. phys. et radium 7, 164 (1946).

<sup>10</sup> G. H. Stafford, Nature 162, 771 (1948).

of wire was 20 cm; it was led through the Kovar-glass seal by a nickel tube of outer diameter 1.5 mm. A purifier of the circulation type was attached to the counter. The gases were introduced into the counter via two needle valves, the moving parts of which were enclosed in bronze siphon bellows so that no grease was in contact with the gas. The counter was always filled with mixtures of argon and deuterium and has operated satisfactorily at pressures up to ten atmospheres of argon plus one-half of an atmosphere of deuterium. The counter was well pumped and flamed; it was then filled to 1 atmosphere with argon, the purifier opened and about 1 cc of sodium dropped inside. The counter was thoroughly pumped and the sodium evaporated by heating. After further pumping at about  $10^{-4}$  mm Hg for a day, the counter was filled; deuterium was put in first. The argon was of the commercial grade known as "oxygen free" and was passed in through a carbon dioxide trap. The deuterium was passed in through palladium. Before the counter was used the gases were circulated; the fresh sodium surface is an excellent purifier,<sup>13</sup> and we have had no trouble from electron attachment.

The work here reported was carried out with a filling of 2 atmospheres each of deuterium and argon; a gas amplification of 5.2 was achieved for an applied voltage of 3960.

#### THE RESOLUTION OF THE PROPORTIONAL COUNTER

The resolution is limited only by the inevitable ballistic spread and by the wall effect; positive ion induction does not occur in the same sense as in the ionization chamber.

The calculation of the wall effect is presented in Appendix IV.

#### THE MEASUREMENT OF THE GAMMA-RAY FLUX

The monitoring of the gamma-ray flux was carried out with a thick-walled brass Geiger counter whose sensitivity, which was checked from day to day with a standard gamma-ray source, did not change by 1 percent over a period of 650 days.

The calculation *ab initio* of the efficiency of a Geiger counter is uncertain and was not attempted; the counter was directly calibrated at 6.14 and 17.6 Mev.

When fluorine is bombarded with protons, many reactions occur. The one of chief concern here consists in the emission of an alpha-particle, leaving the residual nucleus  $O^{16}$  in an excited state at  $6.14 \pm 0.01$  Mev.<sup>14-16</sup>

<sup>13</sup> It is a common fallacy that sodium has a strong affinity for hydrogen; it is difficult to prepare NaH from the two elements by direct combination. We have looked for loss of deuterium over several days, but have found none (the sodium was at room temperature). We are indebted to Dr. A. G. Maddock for telling us of this useful property of sodium.

<sup>14</sup> Strait, Van Patter, Buechner, and Sperduto, Phys. Rev. **81**, 747 (1951).

<sup>15</sup> Hornyak, Lauritsen, Morrison, and Fowler, Revs. Modern Phys. **22**, 291 (1950).

<sup>16</sup> Millar, Bartholomew, and Kinsey, Phys. Rev. **81**, 150 (1951).

If the resonance at a proton energy of 340 kev is used,  $97\frac{1}{2}$  percent of the alpha-particle transitions take place to this state at 6.14 Mev and  $2\frac{1}{2}$  percent to states at 6.9 and 7.1 Mev.<sup>17</sup> No other known gamma-ray emitting states in  $O^{16}$  are accessible. If these alpha-particles are observed at  $90^\circ$  to the proton beam, the relative contribution from alpha-particles making transitions to the ground state of  $O^{16}$  and the pair emitting state at 6.0 Mev is less than 1 percent.<sup>18</sup> Both alpha-particles and gamma-rays are emitted isotropically;<sup>19,20</sup> indeed, strong evidence<sup>21-23</sup> suggests that the level is formed by capture of S-wave protons. The radiative transition from the compound nucleus  $Ne^{20}$  is known<sup>24-26</sup> at a proton bombarding energy of 669 kev, but its intensity is low: it is negligible at the 340-kev resonance. At a bombarding energy of 900 kev the thick target yield of this energetic gamma-ray is roughly 0.2 percent of the 6- and 7-Mev gamma-rays combined.

Some gamma-rays will be internally converted or give rise to internal pair-creation. The 6.14-Mev gamma-ray from the 340-kev level is known to be (probably electric) octupole radiation.<sup>21-23</sup> The conversion coefficients to be expected are very small, being less than  $10^{-6}$  and  $2 \times 10^{-3}$  for internal conversion and pair creation, respectively.<sup>27,28</sup>

It appears that the counting of alpha-particles at  $90^\circ$  to the proton beam constitutes an accurate method of measuring the flux of 6.14-Mev gamma-rays;<sup>29</sup> the alpha-particles preceding the emission of the 6.9- and 7.1-Mev gamma-rays are not counted, but their relative abundance is well known.<sup>17,30</sup> This method was first used by Van Allen and Smith.<sup>31</sup>

The sensitivity of the Geiger counter was determined at 6.14 Mev by counting the alpha-particles with a conventional fast ionization chamber in well-defined geometrical conditions. The natural effect in the Geiger counter and that associated with bombardment of a blank copper disk were respectively  $\frac{1}{2}$  percent and 1 percent of the effect resulting from the  $CaF_2$  target at 33 cm. An inverse square law plot for the Geiger counter is shown in Fig. 1 to a distance from the target of 75 cm. The usual working distance was 33 cm. Loss of alpha-

<sup>17</sup> J. M. Freeman, Phil. Mag. **41**, 1225 (1950).

<sup>18</sup> Streib, Fowler, and Lauritsen, Phys. Rev. **59**, 253 (1941).

<sup>19</sup> J. Van Allen and N. Smith, Phys. Rev. **59**, 501 (1941).

<sup>20</sup> S. Devons and M. G. N. Hine, Proc. Roy. Soc. (London) **A199**, 56 (1949).

<sup>21</sup> W. R. Arnold, Phys. Rev. **79**, 170 (1950).

<sup>22</sup> W. R. Arnold, Phys. Rev. **80**, 34 (1950).

<sup>23</sup> Barnes, French, and Devons, Nature **166**, 145 (1950).

<sup>24</sup> S. Devons and H. G. Hereward, Nature **162**, 331 (1948).

<sup>25</sup> Rae, Rutherglen, and Smith, Proc. Phys. Soc. (London) **A63**, 775 (1950).

<sup>26</sup> J. H. Carver and D. H. Wilkinson, Proc. Phys. Soc. (London) **A64**, 199 (1951).

<sup>27</sup> S. M. Dancoff and P. Morrison, Phys. Rev. **55**, 122 (1939).

<sup>28</sup> M. E. Rose and G. E. Uhlenbeck, Phys. Rev. **48**, 211 (1935).

<sup>29</sup> The distortion of the isotropic distribution by center-of-gravity motion should be considered, but is negligible ( $\sim 0.3$  percent) for observation near  $90^\circ$ .

<sup>30</sup> Chao, Tollestrup, Fowler, and Lauritsen, Phys. Rev. **79**, 108 (1950).

<sup>31</sup> J. Van Allen and N. Smith, Phys. Rev. **59**, 618 (1941).

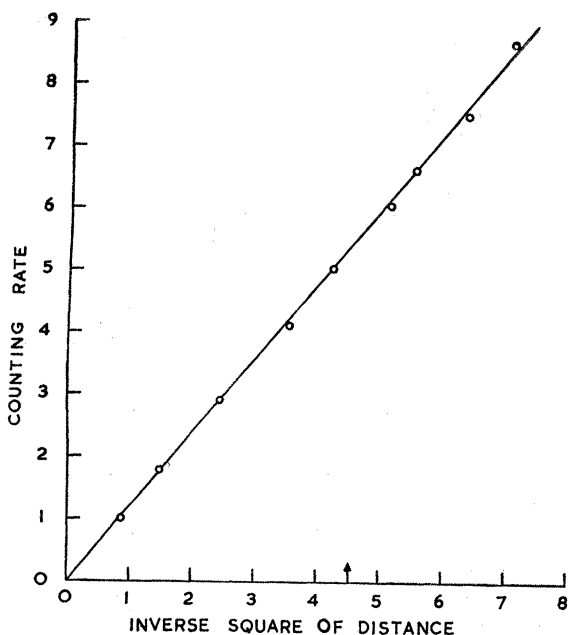


FIG. 1. Inverse square law for the Geiger counter during the alpha-particle calibration. Working point is indicated by the arrow.

particles by single and multiple scattering and their penetration of the edges of the aperture which defined their passage into the counter were computed. These effects were negligible.

The bias curve was analyzed with the help of considerations set out in Appendix V.

Several calibration runs were made over a period of days and a probable error in the calibration of the Geiger counter, based on internal consistency alone, of  $\pm \frac{3}{4}$  percent<sup>32</sup> was determined.

A second calibration was made using a thick-walled current ionization chamber made of graphite, which contained a cylindrical cavity of radius 4.0 cm and depth 2.0 cm filled with pure nitrogen at a pressure of 76 cm Hg. Saturation was fully realized. This method is of common use.<sup>33,34</sup>

The ionization current was translated into gamma-ray flux by the theory of Lax.<sup>35</sup> A correction was computed on account of ionization produced by Compton-scattered photons. This correction amounted to 10 percent for gamma-rays of energy 6.14 Mev<sup>36</sup> and 3 percent for gamma-rays of energy 17.6 Mev. Absorption of gamma-rays in the graphite and surrounding aluminum can was also allowed for as were radiation losses, annihilation of positrons in flight, and the con-

densation effect in graphite.<sup>37-40</sup> The finite size of the cavity was taken into account in the same way as was the finite size of the deuterium chamber. Inverse square plots using various gamma-rays of energy up to 17.6 Mev showed that one may define an effective center of the chamber  $0.45 \pm 0.15$  cm nearer the source than the geometrical center of the cavity.

The energy loss,  $W$  ev, of electrons in forming an ion pair in nitrogen must be known. For fast electrons in air Gray<sup>41</sup> recommends a value of 32.0 ev; the accuracy is about  $\pm 1$  percent. A value for nitrogen may be found in two ways. Firstly, the measurements by Stetter<sup>42</sup> on the ionization produced by the alpha-particles of polonium in various gases suggest a ratio of 1.042 between  $W$  values in nitrogen and air. Secondly, we irradiated the graphite ionization chamber with the same gamma-ray flux both when filled with air and with nitrogen, and thereby derived the value  $1.03 \pm 0.01$  for the preceding ratio. We adopted the value 1.03, obtaining  $W = 32.9$  ev for fast electrons in nitrogen.

Other sources of current are the various photodisintegration processes occurring in the graphite and in the nitrogen. These sources are negligible.

The current chamber was used with the 6.14-Mev gamma-rays from fluorine: it gave a value for their flux lower by  $1\frac{1}{2}$  percent than that given by the counting of alpha-particles. This agreement gave some confidence in the elaborate computations which underlie the results obtained with the current chamber. The result of the alpha-particle calibration was that one count in the brass Geiger counter of wall thickness 0.95 cm, whose sensitive volume was of length 8 cm and diameter 2.6 cm, corresponded to the normal passage per cm<sup>2</sup> across a plane containing the counter's axis of 1.36 quanta of energy 6.14 Mev.

The current chamber was then used to calibrate the Geiger counter for the gamma-rays given by the bombardment of lithium with protons. Radiative capture takes place at a proton energy of about 440 keV, and gamma-rays of 14.8<sup>43</sup> and 17.6 Mev result.<sup>44,45</sup> We take an intensity ratio of 0.55:1 for these two components.<sup>44,46</sup>

<sup>37</sup> E. Fermi, Phys. Rev. **56**, 1242 (1939).

<sup>38</sup> E. Fermi, Phys. Rev. **57**, 485 (1940).

<sup>39</sup> O. Halpern and H. Hall, Phys. Rev. **73**, 477 (1948).

<sup>40</sup> F. L. Hereford, Phys. Rev. **74**, 574 (1948).

<sup>41</sup> L. H. Gray, Proc. Cambridge Phil. Soc. **40**, 72 (1944).

<sup>42</sup> G. Stetter, Z. Physik **120**, 639 (1943).

<sup>43</sup> This lower energy component is known as the 14.8-Mev component after the results of Walker and McDaniel (see reference 44). It is probable that the energy is a little less than this. Walker and McDaniel found the energy to be  $14.8 \pm 0.3$  Mev: Carver and Wilkinson (see reference 26) have measured it as  $14.4 \pm 0.4$  Mev. The best value for the mean position of the level in Be<sup>9</sup> to which the radiative transition occurs is 3.01 Mev (Burcham: private communication), and this corresponds to an energy of 14.60 Mev for the gamma-ray. This value we have used in reducing the results.

<sup>44</sup> R. L. Walker and B. D. McDaniel, Phys. Rev. **74**, 315 (1948).

<sup>45</sup> According to Nabholz, Stoll, and Wäfler, Phys. Rev. **82**, 963 (1951), a gamma-ray of 12.5 Mev is emitted in about 10 percent of the strength of the 17.6 Mev line. This introduces no significant uncertainty in our work.

<sup>46</sup> M. B. Stearns and B. D. McDaniel, Phys. Rev. **82**, 450 (1951).

<sup>32</sup> Throughout this paper  $\pm$  means probable error.

<sup>33</sup> L. H. Gray, Proc. Roy. Soc. (London) **A156**, 578 (1936).

<sup>34</sup> G. C. Laurence, Can. J. Research **A15**, 16 (1937).

<sup>35</sup> M. Lax, Phys. Rev. **A72**, 61 (1947).

<sup>36</sup> This correction comprises 9 percent for the effect of photons which suffer a single Compton scattering and 1 percent for the effect of doubly-scattered photons.

We used a thick target of lithium hydroxide and protons of 510 kev. There is then no inelastic proton scattering in the level in  $\text{Li}^7$  at 453 kev. We found a sensitivity of 0.376 quanta per  $\text{cm}^2$  of 17.6 Mev for one count in the Geiger counter.<sup>47</sup> The intensity ratio may be as high as 0.8:1,<sup>48</sup> the sensitivity would then become 0.372 quanta per  $\text{cm}^2$  of 17.6 Mev per count. We have used 0.55:1.

Our final measurements with the gamma-rays from fluorine were made at a proton bombarding energy of 900 kev. The constitution of the gamma-rays is then 73 parts of 6.14 Mev to 27 parts of 6.9 and 7.1 Mev combined.<sup>17,30</sup> Allowance for this inhomogeneity may accurately be made.

We have made the following estimates of the probable error in our knowledge of the Geiger counter calibration. For the 6.14-Mev gamma-rays,  $\pm\frac{3}{4}$  percent for internal consistency as remarked above;  $\pm 2\frac{1}{2}$  percent in interpretation of the alpha-particle bias curve;  $\pm\frac{2}{3}$  percent for uncertainty in the composition of the gamma-rays at the 340-kev and higher resonances; geometrical errors  $\pm 1\frac{1}{2}$  percent. These errors combine quadratically to  $\pm 3.0$  percent. For the 17.6-Mev gamma-rays, the good agreement of the two methods of flux measurement at 6.14 Mev suggest that  $\pm 5$  percent may be adequate.

These measurements reveal a Geiger counter efficiency increasing a little more rapidly than linearly with gamma-ray energy. For energies below 3 Mev the efficiency of such a counter varies almost linearly with energy.<sup>49</sup> The origin may therefore be used as a third point in the calibration. Little error is involved in

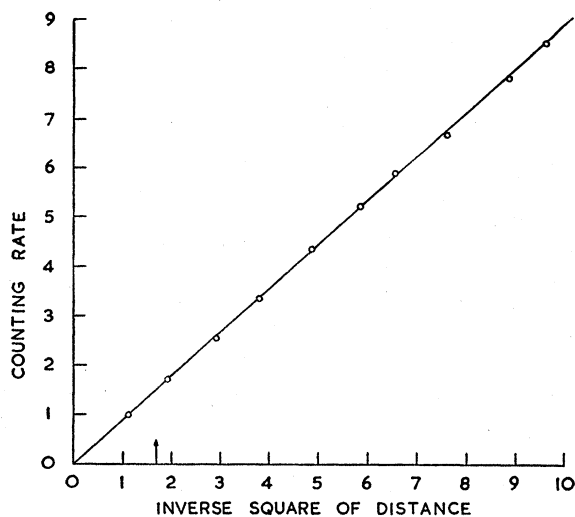


FIG. 2. Inverse square law for the Geiger counter during the disintegration experiment. Normal working point is indicated by the arrow.

<sup>47</sup> Strictly speaking, we derive a sensitivity for the mixed radiation, but the efficiency at the well-defined energy may very rapidly be arrived at by successive approximation.

<sup>48</sup> S. Devons and G. R. Lindsey, Proc. Phys. Soc. (London) A63, 1202 (1950).

<sup>49</sup> J. V. Dunworth, Rev. Sci. Instr. 11, 167 (1940).

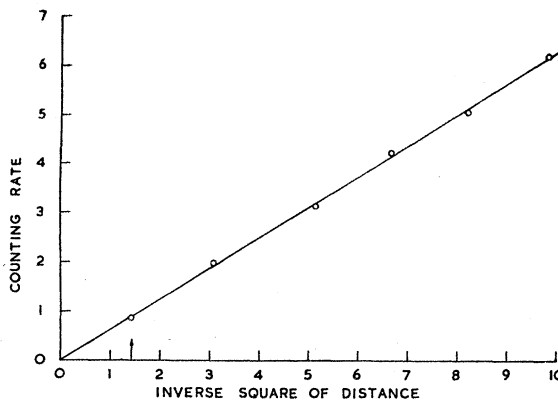


FIG. 3. Inverse square law for the photodisintegration chamber. Normal working point is indicated by the arrow.

estimating efficiencies between the two measured points and an error increasing uniformly from  $\pm 3$  percent at 6 Mev to  $\pm 5$  percent at 18 Mev has been assumed.

For the work at 4.45 Mev we are only interested in the ratio of the Geiger counter efficiency at 4.45 and 6.14 Mev. We have taken an error of  $\pm 2\frac{1}{2}$  percent in this ratio.

#### MEASUREMENTS AT 6.14 MEV

The cross-section measurements with the gamma-rays of 6.14 Mev was preceded by inverse square law investigations both for the Geiger counter and for the deuterium chamber to make sure that scattered radiation was of no importance. A proton energy of 900 kev was used. Figure 2 shows the results for the Geiger counter at distances from the target of 70 to 210 cm. The usual working distance was 172 cm. No background could be detected. Large masses placed near the target had no effect. The pulse distribution from the deuterium chamber was biased off close to the level of electron noise; the inverse square plot is shown in Fig. 3. Again no background could be found. The greatest distance from the target was 59 cm.

A molybdenum shutter could be inserted in the proton beam immediately in front of the target, and by this means we were assured that no significant gamma-ray flux had its origin other than in the fluoride.

Devons and Hine<sup>20</sup> suggest that the gamma-ray flux at  $0^\circ$  to the bombarding proton beam (the direction in which lay the ionization chamber) should be 1.09 in terms of that at  $100^\circ$  (the direction of the Geiger counter) for protons of 900 kev incident upon a thick target; Day, Chao, Fowler, and Perry<sup>50</sup> suggest 1.12 for this quantity. We found a value of 1.11 and adopted it.

The pulse distribution from the deuterium chamber was measured with a ninety-nine channel kick-sorter.<sup>51</sup> Typical distributions are shown in Figs. 4 and 5. Figure 4 is taken at a proton bombarding energy of 500 kev, where the radiation is largely of 6.14-Mev

<sup>50</sup> Day, Chao, Fowler, and Perry, Phys. Rev. 80, 131 (1950).

<sup>51</sup> D. H. Wilkinson, Proc. Cambridge Phil. Soc. 46, 508 (1950).

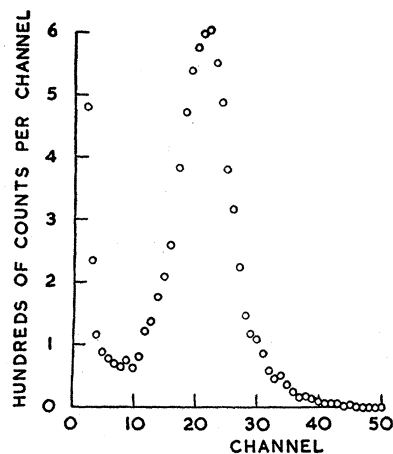


FIG. 4. Photoproton pulse distribution with gamma-rays of 6.14 Mev. Zero of the distribution lies at channel minus 15.

gamma-rays. Figure 5 is taken at 900 kev, where there is a 27 percent admixture of 6.9- and 7.1-Mev components. (The amplifier conditions are not the same for the two figures.) The distribution is noticeably broader in Fig. 5, but no resolution is to be expected in our conditions—the two higher energy peaks would lie at channels 34 and 36.

The possibility that some of these pulses may have been the result of deuterons recoiling from fast neutrons arising in secondary reactions was investigated by means of an ionization chamber identical with that described previously, but filled with ordinary hydrogen instead of deuterium. No significant effect was found.

The pulse distributions were interpreted with the aid of the calculations on resolution and wall effect previously discussed. All the results were corrected for the finite but accurately known dead time (0.0880 second) of the kick-sorter. Five successive runs yielded relative disintegration rates of 1, 1.005, 1.005, 0.979, 1.016; these ratios possess a statistical probable error of  $\pm 0.017$ .

The absorption of gamma-rays between the source and the gas of the ionization chamber is important. It may be calculated,<sup>52</sup> but is of such a magnitude ( $\sim 20$  percent) that we investigated it experimentally. The bulk of the absorption took place in the steel outer wall of thickness 0.67 cm. Other absorbing bodies were the brass target backing (thickness 0.17 cm) and the glass inner envelope of the ionization chamber (thickness 0.2 cm). The absorption in the walls of the ionization chamber is not quite straightforward because some of the quanta which suffer Compton scattering, and which would then be regarded as absorbed on the simple view, in fact still lie above the photodisintegration threshold. The apparent absorption coefficient determined using the ionization chamber as the detector should be a function of the bias setting of the discriminator used to limit the pulse distribution. At zero bias the apparent absorption coefficient should be

<sup>52</sup> W. Heitler, *The Quantum Theory of Radiation* (Oxford University Press, London, 1949).

determined by the pair and photoelectric cross sections plus the Compton cross section for scattering of the gamma-rays below the photodisintegration threshold.

The absorption coefficient was determined by stacking steel plates immediately in front of the ionization chamber. Five plates were used, each of thickness 0.635 cm. A typical absorption curve is shown in Fig. 6. The dotted line indicates the thickness of the steel wall of the ionization chamber. We may not properly expect to be able to define an absorption coefficient at all, but the exponential plot of Fig. 6 shows that this may be done. The factor, derived from such plots, relating the counting rate to be expected without a wall to the chamber with that observed in practice was then determined as a function of discriminator bias; it is displayed in Fig. 7. The bias setting corresponding to the peak of the pulse distribution was 50 volts. The calculated value for "complete" absorption as shown at high bias settings was 1.17, and that for zero bias was 1.12. These figures accord well with the experimental results. The attenuation factor for the pulse size above which the distributions such as those of Figs. 4 and 5 were analyzed in detail was determined from Fig. 7 to be 1.15; the calculated value was 1.15. (In these calculations the form of the dependence of the photodisintegration cross section on gamma-ray energy given by the theory of Bethe and Peierls<sup>7</sup> was used.) The agreement of the experimental and calculated values of the absorption correction means that this correction may be applied with confidence. For all other gamma-rays the absorption correction was calculated. The corrections for absorption in the other bodies mentioned previously were much smaller and were calculated.

#### Results and Errors at 6.14 Mev

The principal errors are<sup>53</sup>  $\pm 3.0$  percent in the gamma-ray flux as previously detailed;  $\pm 2.2$  percent

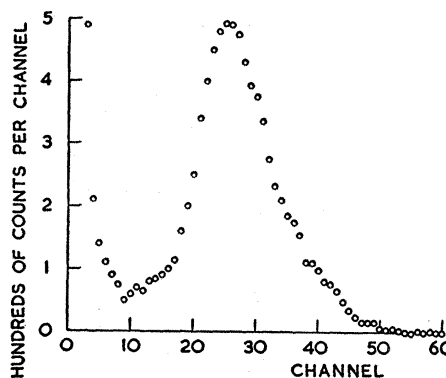


FIG. 5. Photoproton pulse distribution with gamma-rays of 6.14 and 7 Mev. Zero of the distribution lies at channel minus 15.

<sup>53</sup> Where no direct estimate of a probable error was possible but only a maximum tolerance we have adopted one-half of this value as the associated probable error.

for the combined uncertainties in the interpretation of the kick-sorter distribution, wall effect estimate, statistical error in the 12,000 photoprotons counted and error due to the kick-sorter dead time;  $\pm 1.5$  percent for the absorption correction;  $\pm 0.5$  percent for possible Geiger counter fluctuations (the statistical error is negligible);  $\pm 0.35$  percent for geometrical uncertainties;  $\pm 1.5$  percent for uncertainty in the angular distributions;  $\pm 0.3$  percent for possible background radiation in the Geiger counter;  $\pm 0.5$  percent for deuterium pressure;  $\pm 0.5$  percent for deuterium purity.<sup>54</sup> Assembling these errors quadratically we find  $\pm 4.5$  percent as the total probable error in the cross section.

$$\sigma_{6.14} = (21.9 \pm 1.0) \times 10^{-28} \text{ cm}^2.$$

(A correction of 2.5 percent has been made for the mixed character of the gamma-rays. The form of variation of cross section with energy given by Bethe and Peierls<sup>7</sup> was used.)

#### MEASUREMENTS AT 7.39 MEV

When beryllium is bombarded with protons radiative capture takes place in a broad level centered at 998 kev. So far as is known decay takes place directly to the ground state of  $B^{10}$ .<sup>15</sup>

A sharp level formed with protons of 1.087 Mev decays via a state in  $B^{10}$  at 0.713 Mev; the main gamma-ray energy is then about 6.8 Mev. Our proton bombarding energy was 1000 kev and so we remained clear of this double transition. Several more known states in  $B^{10}$  could be involved in double transitions. We have assumed that they are not appreciably excited. It is known from the work of Walker<sup>55</sup> and others, that the low-lying states are not involved in more than a few percent of the strength of the main transition. We are not very sensitive to such transitions, because we should

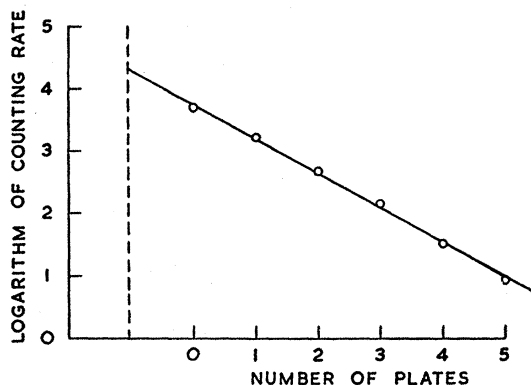
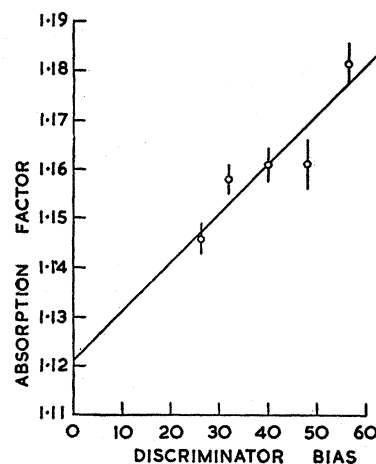


FIG. 6. Absorption curve of 6-Mev radiation in steel plates using the photodisintegration chamber as detector. The thickness of the steel wall of the chamber is indicated by the dotted line.

<sup>54</sup> This purity was measured by the mass spectrograph group at the laboratory of the National Research Council of Canada at Chalk River, Ontario, and found to be 96.98 percent and 96.62 percent on two separate samples of the gas.

<sup>55</sup> R. L. Walker, Phys. Rev. **79**, 172 (1950).

FIG. 7. Absorption factor for the steel wall of the chamber as a function of discriminator bias.



count both the photoprotons and the gamma-rays,<sup>56</sup> and so achieve a large measure of compensation for a small effect. A double transition of considerable danger, however, would be that involving the known state at 3.58 Mev, for we should see almost none of the photoprotons from either gamma-ray. A limit of about 10 percent on the relative probability of this transition is set by the work of Walker<sup>55</sup> (and private communication<sup>57</sup>). We are at the mercy of triple cascades in which the energy is more or less equally shared.

We have considered the production of gamma-rays from several competing reactions and decided that no significant contamination can occur.  $Be^9$  possesses no known excited states below 1 Mev, so inelastic scattering of protons need not be feared.

It was with great annoyance that we discovered, in place of a well-defined photoproton spectrum, the pulse distribution shown in Fig. 8. The photopulse was expected at channel 35.

The explanation of this distressing phenomenon was that a substantial fast neutron flux was being generated. We are dealing with the second-order reactions  $Be^9(p, d)Be^8$  followed by  $Be^8(d, n)B^{10}$  and  $Be^9(p, \alpha)Li^6$  followed by  $Be^9(\alpha, n)C^{12}$ .<sup>58</sup> The former pair is more probable under our conditions.

The run of Fig. 8 had been taken with a thick beryllium target, and the use of a thin target from which the deuterons could escape before losing much energy was demanded. A target of stopping power about 2 kev was used and yielded the pulse distribution shown in Fig. 9. A continuous pulse distribution was still observed, but superposed on it was a clear peak of photoprotons. The neutron spectrum from the two stage process should be closely the same for thick or thin targets; a small correction must be applied to

<sup>56</sup> The Geiger counter has an efficiency roughly proportional to gamma-ray energy and so detects single quantum transitions and cascades with approximately equal efficiency.

<sup>57</sup> We are indebted to Dr. Walker for making this estimate.

<sup>58</sup> The first pair of reactions has been commented on by Jennings, Sun, and Leiter, Phys. Rev. **80**, 109 (1950).



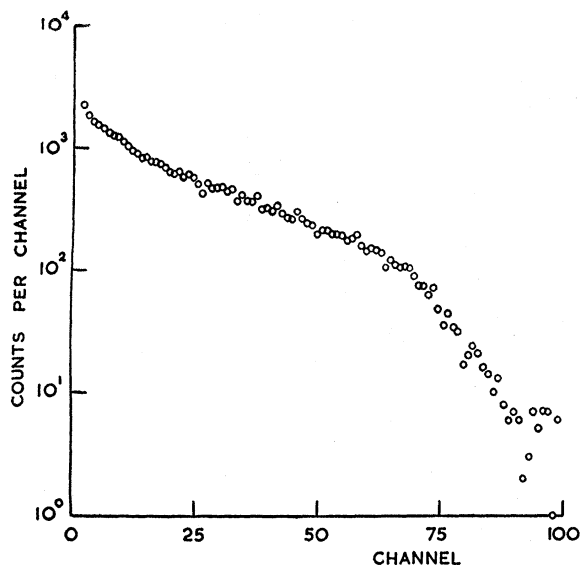


FIG. 8. Pulse distribution from protons of 1000 keV on a thick beryllium target. Zero of pulse distribution at channel minus 16.

the thick target pulse distribution to obtain that for the thin target. This correction was computed with the aid of the known excitation functions of the  $\text{Be}^9(p, d)\text{Be}^8$  and  $\text{Be}^9(d, n)\text{B}^{10}$  reactions and information on the change of neutron spectrum with deuteron energy. This corrected spectrum is shown as the full line in Fig. 9. In the peak the true photoproton counting rate is about five times the background, so the subtraction is not a serious one; when it is made a distribution of the expected shape results. (A small correction is made for the photoproton contribution to the distribution of Fig. 8.) Because of the suspicion always attaching to the subtraction of backgrounds, we have added an extra  $\pm 5$  percent to the error.

Two separate sets of final runs were made, 8 runs in the first set and 9 in the second. Internal consistency within each set was satisfactory, and the two sets agreed to within 3 percent; each contained about 10,000 photoprotons.

During these final runs the chamber was at a distance of 16.9 cm from the target and at  $0^\circ$  to the proton beam. The Geiger counter monitoring was carried out at 44.9 cm and  $45^\circ$ , and the usual corrections for absorption were made. There was a decrease in gamma-ray flux of 5 percent in going from  $45^\circ$  to  $0^\circ$ ; this agrees with the results of Devons and Hine,<sup>20</sup> which lead one to expect a decrease of  $4\frac{1}{2}$  percent.

The gamma-ray yield from excited states of  $\text{B}^{10}$  formed by  $\text{Be}^9(d, n)\text{B}^{10}$  was not big enough to necessitate a correction to the Geiger counter counting rate.

The photoproton peak from the beryllium gamma-rays we locate with an error of  $\pm 1.5$  channels, that from the fluorine calibration gamma-ray to  $\pm \frac{3}{4}$  percent.

The gamma-ray energy is  $7.39 \pm 0.15$  Mev.<sup>59</sup> The mass values predict a gamma-ray energy of 7.39 Mev from the 998-keV resonance.<sup>60</sup> Walker<sup>55</sup> has found an energy of  $7.38 \pm 0.07$  Mev from a thick target and protons of 1.15 Mev, the chief contribution coming from the 998-keV resonance. We have taken 7.39 Mev.

### Results and Errors at 7.39 Mev

Allowances of error above those discussed for the gamma-rays of 6.14 Mev are— $\pm 5$  percent for the subtraction of the neutron background;  $\pm 4$  percent for possible low energy gamma-rays (taking into account the partial compensation for their effects which obtains).

$$\sigma_{7.39} = (18.4 \pm 1.5) \times 10^{-28} \text{ cm}^2.$$

### MEASUREMENTS AT 8.14 MEV

The radiative capture of protons by  $\text{C}^{13}$  in the resonance level at a proton energy of 554 keV gives a single quantum of about 8.1 Mev by a transition to the ground state of  $\text{N}^{14}$ . There is also a possible competing transition to the state in  $\text{N}^{14}$  at about 2.3 Mev. Lauritsen and Fowler<sup>61</sup> using a thick target report that these alternative transitions take place with equal intensity and find no other gamma-rays. Day<sup>62</sup> and Woodbury<sup>63</sup> find no evidence for the double cascade but an indication of a triple cascade of intensity about 13 percent of that of the direct transition. We are again sensitive to multiple transitions and the general remarks made previously in connection with the beryllium gamma-rays apply. However, we would have seen evidence of any other double transition of strength more than a percent or two of the 8.1-Mev line. Such transitions were not detected and, if present, would also be quite well compensated for; this is so even if they involved the state at 3.9 Mev almost midway between the initial and ground states, because the "electron-noise" cut-off does not occur until an equivalent gamma-ray energy of 4.2 Mev. We have assumed a 13 percent contribution of triple cascades in reducing the gamma-ray flux.

There are here no competing reactions and inelastic proton scattering need not be considered as no suitable levels are known in  $\text{C}^{13}$ .<sup>15</sup>

A target of  $\text{C}^{13}$  deposited on copper was bombarded with protons of 570 keV;<sup>64</sup> its thickness was estimated

<sup>59</sup> A notice of the gamma-ray energies derived in this work has been published by Carver and Wilkinson (see reference 26).

<sup>60</sup> No allowance for Doppler shift has been made in any of the calculated gamma-ray energies; the shift is never as much as  $\frac{1}{2}$  percent.

<sup>61</sup> T. Lauritsen and W. A. Fowler, *Phys. Rev.* **58**, 193 (1940).

<sup>62</sup> Private communication.

<sup>63</sup> Ph.D. thesis. California Institute of Technology (1951).

<sup>64</sup> The resonance is centered at 554 keV and has a width at half-maximum of about 40 keV. We have sacrificed yield in working at 570 keV in order to keep away from the radiative capture resonance in  $\text{C}^{12}$  at 453 keV (width 35 keV). Our target was electromagnetically separated and so should be very free of  $\text{C}^{12}$ , but another source is deposition onto the target from oil of the diffusion pumps. All our other work, with the exception of



from the yield and reaction constants<sup>65</sup> as 20 kev, and so the effective proton energy was about 560 kev.

The ionization chamber was irradiated at 0° to the proton beam and at a distance from the target of 18.9 cm. The Geiger counter monitoring was done at 40° and 42.6 cm. The pulse distribution on which the estimate of the cross section was based is shown in Fig. 10. It is at once obvious that there is only one strong component in the gamma-ray spectrum. The ratio of width at half-maximum to peak position should be almost constant for our photoproton groups. This ratio for fluorine gamma-rays is about 0.28; for the main peak of Fig. 10 it is 0.29, demonstrating that this peak is not a superposition of two due to gamma-rays of significantly different energy. Some lower energy line is present; the photoprotons below the main group are only partly explained as wall effect. We determined the shape of the electron noise spectrum several channels below the zero of Fig. 10; this enabled us to extrapolate the noise into the region of the spectrum displayed in Fig. 10. The best account of the observed pulse distribution was given by a second line at about 5.8 Mev, whose intensity was 0.07 in terms of that of the 8.1-Mev line. The combined effects of these two lines plus their wall effects, and the extrapolated electron noise are shown by the dotted line. It is seen that this gives a decent account of the experimental points

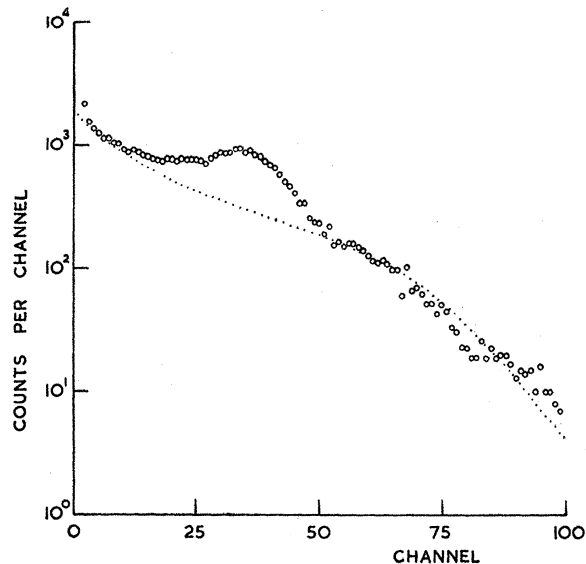


FIG. 9. Pulse distribution from protons of 1000 kev on a thin beryllium target. Zero of pulse distribution at channel minus 16.

some using lithium, where the deposition of even a thick target of carbon would have been unimportant, has been carried out either at proton energies well below 450 kev or well above, where the deposit of a thin target of carbon would have no effect. Here we are constrained to work relatively close to the C<sup>13</sup> resonance. The constancy in apparent position of the C<sup>13</sup> resonance, and the internal consistency of the results show that if any carbon built up during the work, it did not have any effect.

<sup>65</sup> Fowler, Lauritsen, and Lauritsen, *Revs. Modern Phys.* **20**, 236 (1948).

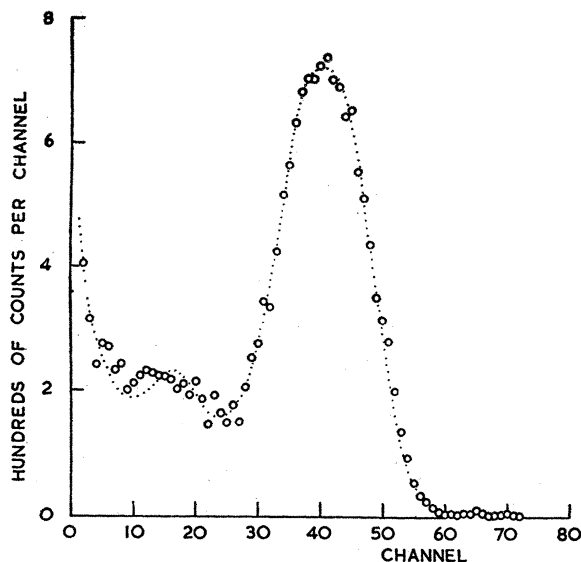


FIG. 10. Photoproton pulse distribution from protons of 570 kev on a "medium thin" target of C<sup>13</sup>. Zero of pulse distribution at channel minus 20. Dotted curve "theoretical"—see text.

except, perhaps, for a few around channel 10. If a third line were present, its energy would be about 5.2 Mev, and its intensity about 0.015 of that of the 8.1-Mev line. This possibility is of little consequence for the absolute cross section.

There were four final runs; each contained about 3500 pulses and the relative yields of disintegrations per Geiger counter count were 1:0.98:0.98:1.01.

No correction was found necessary for angular distribution, and the absorption was calculated in the usual way.

The main peak we locate with an accuracy of  $\pm 0.7$  channels, the subsidiary peak to  $\pm 2.5$  channels and the calibrating fluorine peak to  $\pm \frac{3}{4}$  percent. The gamma-ray energies are  $8.14 \pm 0.08$  and  $5.81 \pm 0.25$  Mev. From the mass values we expect, for the main line, 8.08 Mev. Lauritsen and Fowler<sup>61</sup> report  $8.1 \pm 0.2$  Mev for this line. We have adopted 8.14 Mev.

It is possible that the lower energy line is the result of fluorine contamination; if this is so, the difference made to the final cross section is less than 1 percent.

#### Results and Errors at 8.14 Mev

We must again allow for the uncertainty in our knowledge of low energy components in the gamma-rays. The 13 percent strength of the triple cascade is not very accurate, and we have added  $\pm 4$  percent to our error on this account.

$$\sigma_{8.14} = (18.0 \pm 1.3) \times 10^{-28} \text{ cm}^2.$$

#### MEASUREMENTS AT 12.5 MEV

The radiative capture of protons by B<sup>11</sup> provides gamma-rays of about 17 Mev by a transition to the ground state of C<sup>12</sup>. More usually, a double transition

is made via the state in  $C^{12}$  at 4.45 Mev, and it is the gamma-ray of about 12.5 Mev associated with this cascade which we have used in the present work. Unfortunately the reaction is not resonant around 1-Mev proton energy, so conditions are not so well defined as in the earlier work. With protons of 900 kev and a thick target, Fowler, Gaerttner, and Lauritsen<sup>66</sup> report single transitions and cascades in the ratio 0.15:1. Walker<sup>55</sup> gives for this ratio at proton energies of 510 kev and 1.2 Mev (thick target), 0.25:1 and 0.48:1, respectively. Rutherglen<sup>67</sup> suggests 0.19:1 at 700 kev. It is evident<sup>55</sup> that other cascades are not very frequent.

The reaction  $B^{11}(p, \alpha)Be^8$  does not result, so far as is known, in any gamma-radiation as the bulk of the transitions go to the state at about 3 Mev in  $Be^8$  which decays by alpha-particle emission. That only a small number of transitions go to the gamma-ray emitting state at 4.9 Mev in  $Be^8$  is shown by the approximate equality which all workers find in the intensities of the 4.45-Mev and 12.5-Mev components. The first excited state in  $B^{11}$  is at 2.14 Mev, so inelastic proton scattering need not be considered. Another source of gamma-rays is the  $B^{10}$  contained in our natural boron target. There is little radiative capture; it has been observed by Walker<sup>55</sup> with a resonance at a proton energy of 1.16 Mev. The reaction  $B^{10}(p, \alpha)Be^7$  is a source of gamma-rays of 0.43 Mev on account of the strong transition to the first excited state of  $Be^7$ . The correction was estimated for our experimental conditions by measuring the Geiger counter counting rate on bombarding a target of separated  $B^{10}$ ; it was a little less than 10 percent.

A target of thickness about 200 kev was prepared by sedimentation of natural boron powder, and bombarded with protons of 950 kev. As with the thick beryllium target, there was no sign of a photoproton peak. The explanation is of the same type as before: the alpha-particles from  $B^{11}(p, \alpha)Be^8$  act upon further boron

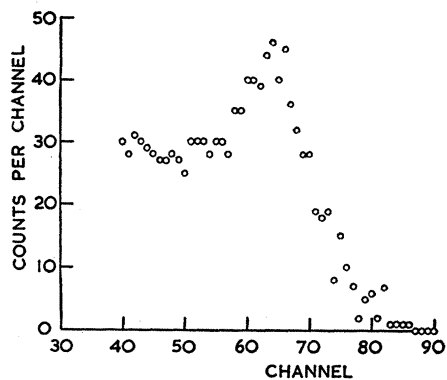


FIG. 11. Pulse distribution from the bombardment of boron with protons of 950 kev and 15 cm of paraffin wax interposed between source and ionization chamber. Zero of pulse distribution at channel minus 15.

<sup>66</sup> Fowler, Gaerttner, and Lauritsen, *Phys. Rev.* **53**, 628 (1938).

<sup>67</sup> Private communication.

nuclei, giving neutrons. The same remedy of using a very thin target could not be applied, for  $B^{11}(p, \gamma)C^{12}$  is not resonant and the gamma-ray yield was low. Instead 15 cm of paraffin wax was placed between the target and the ionization chamber to scatter the neutrons. A pulse distribution, which revealed a high energy peak, was obtained; it is shown in Fig. 11. Some pulses below the peak are still caused by neutrons, but we know from the distribution without wax that if there is an appreciable number at channel 45 then there will be very few in the peak itself. We have no reliable subtraction recipe, and knowledge of the disintegration rate comes from the peak alone, which is due to the line at 12.5 Mev. The intensity of the line at about 17 Mev is low, and the pulses due to it would be almost all "wall-effect;" we should not then expect to see this line. An allowance for the contribution of the higher energy line to the peak must be made. Although the estimate of the disintegration rate due to 12.5-Mev gamma-rays varies with the assumed strength of the direct transition, the final answer for the cross section at 12.5 Mev does not vary much because, as we increase the percentage of the 17-Mev line and reduce the number of pulses in the peak to be ascribed to the 12.5-Mev line, so do we also reduce the gamma-ray flux associated with the 12.5-Mev line.

During the runs with wax the chamber was at a distance of 33 cm from the target and at  $0^\circ$  to the proton beam. The Geiger counter monitoring was carried out at 73 cm and  $45^\circ$ .

Six final runs were made, but the counts were so few in each that individual analysis was not profitable.

Combined allowance for angular distribution and gamma-ray absorption in the wax was made by comparing the counting rate of the Geiger counter in the monitoring position and at  $0^\circ$  (but at a distance of 2 meters, so that "good geometry" was achieved and the Compton scattered gamma-rays ignored).

The peak of Fig. 11 we locate to  $\pm 1.5$  channels, the fluorine calibration peak to  $\pm \frac{3}{4}$  percent; the resulting gamma-ray energy is  $12.50 \pm 0.21$  Mev. The energy expected for the direct transition from the mass tables at a proton energy of 900 kev is 16.75 Mev. The first excited state in  $C^{12}$  is at 4.46 Mev, and so the expected value of the energy for the first element of the cascade is 12.29 Mev. Other measurements are by Fowler, Gaerttner, and Lauritsen,<sup>66</sup> who obtained  $11.8 \pm 0.5$  Mev from a thick target and protons of peak energy 0.9 Mev, and by Walker<sup>55</sup> who quotes  $11.76 \pm 0.18$  Mev for protons of 0.51 Mev and  $12.12 \pm 0.12$  Mev for protons of 1.15 Mev, both with thick targets. We have adopted 12.50 Mev.

### Results and Errors at 12.5 Mev

This is a bad experiment. The errors introduced by our uncertainty of the constitution of the gamma-rays are small compared with the others. We have taken a probable error of  $\pm 7$  percent in the disintegration rate,

an additional  $\pm 3$  percent on account of the absorption of the gamma-rays in the wax, and  $\pm 2$  percent for the  $B^{10}$  correction. This gives a total error of  $\pm 10$  percent

$$\sigma_{12.5} = (10.4 \pm 1.0) \times 10^{-28} \text{ cm}^2.$$

#### MEASUREMENTS AT 17.6 MEV

We have already discussed the gamma-rays emitted in the radiative capture of protons of 510 kev by  $\text{Li}^7$ . When they were used to irradiate the deuterium chamber, strong effects caused by fast neutrons were again in evidence. These neutrons arise from two sources. In the first the alpha-particles produced in the reaction  $\text{Li}^7(p, \alpha)\text{He}^4$  act upon the lithium of the target; in the second the gamma-rays give  $(\gamma, n)$  reactions in the material of the laboratory and ionization chamber.

The second source was the stronger under our experimental conditions.  $(\gamma, p)$  reactions which could occur in the glass walls of the ionization chamber were considered, but may be neglected in our conditions. The high pressure hydrogen chamber was used to estimate the fast neutron background. The cross section for neutron collision, the energy transfer, and the angular distribution of recoil particles are all different for protons and deuterons. The use of the hydrogen chamber would therefore be unjustified but for a happy circumstance. We irradiated the two chambers identically with neutrons from a radium-beryllium source. These neutrons possess an extended neutron spectrum somewhat similar in range to that which must arise in  $(\gamma, n)$  reactions. The pulse distributions were measured and compared; when a suitable adjustment in scale had been made, they were indistinguishable over a considerable range at high energy.

The hydrogen chamber was then used to investigate the lithium "gamma-rays." The resulting distribution was treated according to the recipe derived from the neutron irradiations and subtracted from the distribution given by the deuterium chamber. Over the narrow range of subtraction recipes permitted by the data obtained with the radium-beryllium neutrons, the final subtracted photodisintegration distribution was almost unchanged. This fact lends confidence in the subtraction procedure, as does a comparison of the subtracted distribution with that calculated. The calculated distribution was smoothed and then "smeared" using the appropriate Gaussian distribution representing the amplifier and gamma-ray noise. As the wall effect was large a complete numerical integration was performed, taking into account the measured width of 2 Mev of the 14.8-Mev line as reported by Walker and McDaniel.<sup>44</sup> The result was, however, quite close to that given by the analytical formulas suitably modified to take account of inductive effects in the partial tracks. This modification is necessary at high gamma-ray energy where the tracks are very long and no longer confined to the region of the chamber near the wall where the inductive effects are small as they are for

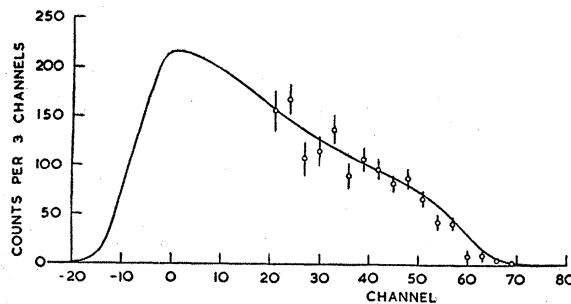


FIG. 12. Observed and calculated photoproton distributions for the gamma-rays from lithium. Zero of the distribution lies at channel minus 9.

the lower energy gamma-rays. The calculated distribution is shown by the full line of Fig. 12. The experimental points have been grouped at intervals of three channels; the probable errors are purely statistical.

The number of photodisintegrations was determined with a probable error which was estimated at  $\pm 10$  percent by the extreme fittings of calculated and experimental distributions. There was no angular distribution correction.

#### Results and Errors at 17.6 Mev

The greatest error is the  $\pm 10$  percent for the fitting of observed and calculated distributions. The other errors increase this to  $\pm 12$  percent. The uncertainty in the composition of the gamma-rays is not very important; if the ratio of 14.8 to 17.6 Mev lines were as great as 0.8:1, the cross section would be lowered by only  $4\frac{1}{2}$  percent.

$$\sigma_{17.6} = (7.7 \pm 0.9) \times 10^{-28} \text{ cm}^2.$$

(Again we have corrected for the lower energy line using the form of dependence of cross section on energy given by Bethe and Peierls.<sup>7</sup>)

#### MEASUREMENTS AT 4.45 MEV

When  $\text{N}^{15}$  is bombarded with protons of about 1 Mev, the reaction  $\text{N}^{15}(p, \alpha)\text{C}^{12}$  takes place; it is similar to the reaction  $\text{F}^{19}(p, \alpha)\text{O}^{16}$  in that at some resonances nearly all transitions leave the residual nucleus in an excited state.<sup>68</sup> We have used the resonance at a proton energy of 898 kev. The excited state in  $\text{C}^{12}$  is at about 4.5 Mev. It is believed that no excited states in  $\text{C}^{12}$  lie below 4.5 Mev;<sup>15</sup> neither are there accessible states above the one we use.

Radiative capture must be considered, it is reported<sup>68</sup> in a broad state around 1.0 Mev, giving gamma-rays of about 13 Mev. This transition is insignificant relative to the desired one at a proton energy of 900 kev which we used. We failed to find it with the high pressure chamber. There are no other competing reactions, and not even the ground-state alpha-particles can give the reaction  $\text{N}^{15}(\alpha, n)\text{F}^{18}$ . It was decided to measure

<sup>68</sup> Schardt, Fowler, and Lauritsen, Phys. Rev. **80**, 136 (1950).

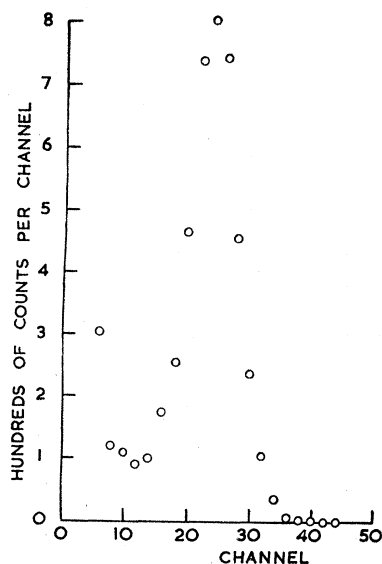


FIG. 13. Pulse distribution given by the proportional counter from protons of 890 kev on  $N^{15}$ . Zero of the distribution lies at channel minus 12.

the cross section at 4.45 Mev relative to that at 6.14 Mev.

The target was of  $N^{15}$  electromagnetically separated into molybdenum; it was effectively thin and on bombardment with protons of 890 kev it gave a just-adequate supply of the desired gamma-rays. The proportional counter was set up at  $0^\circ$  to the proton beam and 6.8 cm away from the target. The Geiger counter was at 19.6 cm and  $115^\circ$ . A typical pulse distribution is shown in Fig. 13. The ratio of width<sup>69</sup> at half-maximum to peak position is now 0.18 as against 0.28 for the pressure chamber; the value of this ratio expected from the ballistics of the reaction alone is 0.14. Similar results were obtained with fluorine irradiations at the 340-kev resonance which were interwoven with the  $N^{15}$  runs, and for which the proportional counter was set up in exactly the same position relative to the target. Four  $N^{15}$  runs were made, each containing about 1200 pulses. They bore relative yields per Geiger counter count of 1:1.05:1.02:1.05. The fluorine runs contained many more pulses. We believe that the relative yields of photoprotons have been determined to  $\pm 2$  percent in the statistics and  $\pm 2$  percent on account of the wall effects.

Another source of error was the large anisotropy which was found in the angular distribution of the gamma-rays; it could be roughly represented by  $1+0.3 \cos^2\theta$  though it rose more rapidly than this towards  $0^\circ$ . This necessitated a numerical integration over the volume of the proportional counter. We have increased the error by  $\pm 2$  percent on this account.

Two separate sets of  $N^{15}$  and  $F^{19}$  runs were compared to find the gamma-ray energy. In the first set the  $N^{15}$  peak was located to  $\pm 0.1$  channels (in 14), and the  $F^{19}$  peak to  $\pm 0.15$  channels (in 24), in the second set the

<sup>69</sup> This width includes gas amplification and amplifier drifts over two hours.

errors were  $\pm 0.2$  channels (in 26) and  $\pm 0.3$  channels (in 45). The two sets agreed well and the resulting gamma-ray energy is  $4.45 \pm 0.04$  Mev. This gamma-ray energy has been measured in the same reaction by Thomas and Lauritsen,<sup>70</sup> who find  $4.465 \pm 0.02$  Mev. Estimates of the location of the level in  $C^{12}$  come from other sources. Schardt, Fowler, and Lauritsen<sup>68</sup> have measured the  $Q$  value of the short-range alpha-particle reaction as  $0.529 \pm 0.008$  Mev; Strait *et al.*<sup>14</sup> have measured the  $Q$ -value of the ground-state transition as  $4.960 \pm 0.007$ ; these measurements locate the state at  $4.431 \pm 0.011$  Mev. Bradford and Bennett<sup>71</sup> locate the state at 4.45 Mev by a study of neutron groups from  $Be^9(\alpha, n)C^{12}$ ; Pringle, Roulston, and Standil<sup>72</sup> report a gamma-ray of  $4.40 \pm 0.05$  Mev, and Terrell<sup>73</sup> one of  $4.45 \pm 0.09$  Mev from the same reaction. We have adopted 4.45 Mev.

### Results and Errors at 4.45 Mev

All sources of error have been mentioned and we find

$$\sigma_{4.45}/\sigma_{6.14} = 1.11 \pm 0.06.$$

This result, combined with that quoted above for  $\sigma_{6.14}$ , gives

$$\sigma_{4.45} = (24.3 \pm 1.7) \times 10^{-28} \text{ cm}^2.$$

### COLLECTED RESULTS

We gather together the gamma-ray sources, the value of the gamma-ray energy, and the total cross section. (See Table I.) The gamma-ray energy from fluorine is derived as explained previously, that from lithium is due to Walker and McDaniel,<sup>44</sup> and the rest are our own values based on the fluorine gamma-ray as standard. These results have already been published in preliminary form by Barnes, Stafford, and Wilkinson,<sup>74</sup> and by Carver and Wilkinson.<sup>75</sup> Few other measurements exist in this range of gamma-ray energy. They are summarized in Table II.<sup>76-78</sup>

### ACKNOWLEDGMENTS

We would like to thank Dr. W. B. Lewis and the staff of the mass spectrometer group at the laboratory of the National Research Council of Canada, Chalk River, Ontario, for their analysis of the deuterium; Dr. C. Sykes, of Messrs. Firth-Brown, Sheffield, who supplied and heat-treated the steel from which the outer shells of the ionization chambers were made; Sir John Cockcroft and Dr. J. V. Dunworth, of the Atomic Energy Research Establishment, Harwell, for the graphite from which the graphite ionization chamber was made; Sir

<sup>70</sup> R. G. Thomas and T. Lauritsen, quoted in reference 15.

<sup>71</sup> C. E. Bradford and W. E. Bennett, *Phys. Rev.* **78**, 302 (1950).

<sup>72</sup> Pringle, Roulston, and Standil, *Phys. Rev.* **78**, 627 (1950).

<sup>73</sup> J. Terrell, *Phys. Rev.* **80**, 1076 (1950).

<sup>74</sup> Barnes, Stafford, and Wilkinson, *Nature* **165**, 69 (1950).

<sup>75</sup> J. H. Carver and D. H. Wilkinson, *Nature* **167**, 154 (1951).

<sup>76</sup> Phillips, Lawson, and Kruger, *Phys. Rev.* **80**, 326 (1950).

<sup>77</sup> P. V. C. Hough, *Phys. Rev.* **80**, 1069 (1950).

<sup>78</sup> H. Wäffler, Report to Chicago Conference (1951).

John Cockcroft and Dr. W. D. Allen for supplying us with the separated isotopes of many elements.

C. A. Barnes, J. H. Carver, and G. H. Stafford wish to thank respectively the Commissioners of the Exhibition of 1851 and the National Research Council of Canada; the Australian National University; the University of Cape Town and the South African C.S.I.R. for grants received in connection with this work.

### APPENDIX I

#### Inductive Effects between Confocal Ellipsoids

Point ionizing events occur uniformly throughout the volume between two confocal ellipsoids; the outer ellipsoid, the cathode, has the form

$$\frac{x^2}{\lambda_0^2} + \frac{y^2+z^2}{\lambda_0^2-1} = 1;$$

the inner ellipsoid, the anode, has the form

$$\frac{x^2}{\lambda_i^2} + \frac{y^2+z^2}{\lambda_i^2-1} = 1 \quad 1 < \lambda_i < \lambda_0.$$

The  $x$  axis is defined by the major axis of the anode. The result for the pulse distribution is most easily expressed in terms of  $B(P)$ , the probability that a pulse will exceed the relative size  $P$ . Neglecting the volume of the anode relative to that of the cathode,

$$B(P) = 1 - \frac{4XY^P(1+XY^P)}{(1-XY^P)^3} \cdot \frac{1}{(\lambda_0^2-1)\lambda_0},$$

where

$$X = \frac{\lambda_i^2-1}{(\lambda_i+1)^2} \quad Y = \frac{\lambda_0^2-1}{\lambda_i^2-1} \left\{ \frac{\lambda_i+1}{\lambda_0+1} \right\}^2.$$

### APPENDIX II

#### Ballistic Spread with Induction

Photodisintegration takes place uniformly between coaxial cylinders, the larger, the cathode, of radius  $b$ , the anode of radius  $a$ . Electric dipole transitions take place which, in the absence of induction, would yield a differential energy distribution

$$P(E) = 1 - (E-M)^2/K, \quad P \geq 0$$

(the normalizing factor is omitted). The proton energy is  $E$ ;  $M = \frac{1}{2}(h\nu - \epsilon)$ ;  $h\nu$  is the energy of the gamma-ray

TABLE I. Gamma-ray energies and deuteron photodisintegration cross sections.

Reaction	Gamma-ray energy (Mev)	Cross section ( $\times 10^{28}$ cm <sup>2</sup> )
N <sup>15</sup> ( $\beta, \alpha$ )C <sup>12</sup> *	4.45 $\pm$ 0.04	24.3 $\pm$ 1.7
F <sup>19</sup> ( $\beta, \alpha$ )O <sup>16</sup> *	6.14 $\pm$ 0.01	21.9 $\pm$ 1.0
Be <sup>9</sup> ( $\beta, \gamma$ )B <sup>10</sup>	7.39 $\pm$ 0.15	18.4 $\pm$ 1.5
C <sup>13</sup> ( $\beta, \gamma$ )N <sup>14</sup>	8.14 $\pm$ 0.08	18.0 $\pm$ 1.3
B <sup>11</sup> ( $\beta, \gamma$ )C <sup>12</sup> *	12.50 $\pm$ 0.21	10.4 $\pm$ 1.0
Li <sup>7</sup> ( $\beta, \gamma$ )Be <sup>8</sup>	17.6 $\pm$ 0.2	7.7 $\pm$ 0.9

TABLE II.

Workers	Gamma-ray energy (Mev)	Cross section ( $\times 10^{28}$ cm <sup>2</sup> )
Van Allen and Smith <sup>a</sup>	6.2	11.6 $\pm$ 1.5
Phillips, Lawson, and Kruger <sup>b</sup>	6.14	26.9 $\pm$ 3.8
Hough <sup>c</sup>	17.6	7.2 $\pm$ 1.5
Waffler <sup>d</sup>	17.6	7.1 $\pm$ 2.0

<sup>a</sup> See reference 31. <sup>b</sup> See reference 76. <sup>c</sup> See reference 77. <sup>d</sup> See reference 78.

and  $\epsilon$  is the binding energy of the deuteron.

$$K = \frac{h^2\nu^2}{4mc^2} \left( h\nu - \epsilon - \frac{h^2\nu^2}{4mc^2} \right),$$

where  $m$  is the proton or neutron mass.

When induction is taken into account we obtain the distorted distribution

$$D(E) = \left[ \bar{\text{Ei}}(x)(A+B+C) - \frac{e^x}{x} \times \left( B+C \left( 1 + \frac{1}{x} \right) \right) \right] \frac{(E/L) \log(b^2/a^2)}{(E/E_{\text{max}}) \log(b^2/a^2)}$$

(again the normalizing factor is omitted), where

$$\bar{\text{Ei}}(x) = \int_{-\infty}^x e^z/z dz \quad (\text{tabulated by Jahnke and Emde}^{79})$$

$$A = K - M^2, \quad B = 2ME \log(b^2/a^2),$$

$$C = -\frac{1}{2}(E \log(b^2/a^2))^2, \quad E_{\text{max}} = M + \sqrt{K}.$$

The limit  $L$  is  $E_{\text{min}}$ , that is  $M - \sqrt{K}$ , for  $E < E_{\text{min}}$ , and  $E$  for  $E_{\text{min}} \leq E \leq E_{\text{max}}$ .

### APPENDIX III

#### The Wall Effect in a Spherical Chamber

If infinitely long tracks originate at random throughout a sphere of radius  $r$  then, independent of their angular distribution relative to any specified direction, the probability  $p(l)dl$  that any track should have a length  $l$  to  $l+dl$  before striking the wall is given by

$$p(l) = (3/4r)[1 - (l/2r)^2].$$

If the tracks have a maximum length of  $l_0$ , a fraction

$$\Phi_0 = 1 - (3l_0/4r)(1 - l_0^2/12r^2)$$

does not hit the wall. If we make the approximation that all the proton tracks have the same range, appropriate to the mean energy  $M$ , we distribute a fraction  $\Phi_0$  within the group whose form we have stated in Appendix II. The remainder is distributed according to the amount of their track which lies in the gas. No correction for positive ion induction effects need in general be made since these partial tracks lie near the wall where the induction is small. When  $\Phi_0$  becomes small, however, the induction effects play an appreci-

<sup>79</sup> E. Jahnke and F. Emde, *Tables of Functions* (Dover Publications, New York, 1945).

able rôle in modifying the shape of the distribution curve, and must be allowed for, as also must the real initial energy distribution of the protons. An approximation to the range-energy relation may be made in the form  $R = cE^S$ ,  $R$  is the range of the particle. For hydrogen  $S = 1.77$  gives a good approximation in the energy range covered in this work.<sup>80</sup> If the probability is  $\Phi(f)df$  that a proton spends a fraction  $f$  to  $f+df$  of its energy in the chamber gas,

$$\Phi(f) = \frac{3}{4}S(M/E_r)^S(1-f)^{S-1} \times \{1 - \frac{1}{4}(M/E_r)^{2S}[1 - (1-f)^S]^2\},$$

where  $E_r$  is the energy of a proton whose range is equal to the radius of the chamber; this was 5.14 Mev.

#### APPENDIX IV

##### The Wall Effect in a Cylindrical Chamber

Gamma-rays are incident at right angles to the axis of an infinitely long cylinder of radius  $r$  and produce photodisintegrations by electric dipole transitions (the angular distribution is here of importance). The corrections because of the finite length of the counter are easily made and will not be discussed.

Let  $f = l/2r$ , where  $l$  is the residual track length in the chamber. We then seek  $p(f)$ , where  $p(f)df$  is the probability that an infinitely long track should have a length  $f$  to  $f+df$  contained within the cylinder.

$$p(f) = \frac{3}{\pi} \int_0^{\alpha_0} \sin^2 \alpha (1 + \cos^2 \alpha) (1 - f^2 \sin^2 \alpha)^{\frac{1}{2}} d\alpha$$

where

$$\begin{aligned} \alpha_0 &= \pi/2, \quad 0 \leq f \leq 1 \\ &= \sin^{-1}(1/f), \quad 1 < f. \end{aligned}$$

This integral gives a solution in terms of closed elliptic integrals of the first and second kind (tabulated by Jahnke and Emde<sup>79</sup>). For  $0 \leq f \leq 1$

$$p(f) = \frac{3}{\pi f^2} \left\{ K(f) \left[ 2(1-f^2) - \frac{3}{5f^2}(1+2f^2)(1-f^2) \right] - E(f) \left[ 2(1-2f^2) - \frac{1}{5f^2}(2+3f^2-8f^4) \right] \right\}.$$

For  $1 < f$ , setting  $g = 1/f$ ,

$$p(f) = \frac{1}{5\pi g} \left\{ K(g)(-12+13g^2-g^4) - E(g)(-12+7g^2-2g^4) \right\},$$

where

$$\begin{aligned} K(h) &= \int_0^{\pi/2} \frac{d\theta}{(1-h^2 \sin^2 \theta)^{\frac{1}{2}}} \\ E(h) &= \int_0^{\pi/2} (1-h^2 \sin^2 \theta)^{\frac{1}{2}} d\theta. \end{aligned}$$

<sup>80</sup> H. A. Bethe, *Range-Energy Curves*, Brookhaven National Laboratory Report No. T-7 (1949).

For  $f \ll 1$  asymptotic expressions for the elliptic integrals give expressions which are quite accurate throughout the range of  $f$ . The fraction of disintegrations which result in a track of length less than  $P$  is  $P(f)$ .

For  $0 \leq f \leq 1$

$$p(f) = \frac{1}{16} \left( 15 - \frac{21}{4}f^2 - \frac{135}{128}f^4 \right)$$

$$P(f) = \frac{f}{16} \left( 15 - \frac{7}{4}f^2 - \frac{27}{128}f^4 \right).$$

For  $1 < f$

$$p(f) = \frac{1}{40f^3} \left( 15 + \frac{75}{128} \frac{1}{f^4} \right)$$

$$P(f) = 1 - \frac{1}{80f^2} \left( 15 + \frac{75}{384} \frac{1}{f^4} \right).$$

At  $f = 1$  the expression valid for  $f \ll 1$  and that valid for  $f \gg 1$  differ by less than  $\frac{1}{2}$  percent. To compute the energy distribution we have used the data of Bethe<sup>80</sup> for deuterium and of Hirschfelder and Magee<sup>81</sup> for argon.

#### APPENDIX V

##### The Alpha-Particle Bias-Curve Plus Noise

Owing to the finite size of the fast ionization chamber used to count the alpha-particles, there exist inductive effects which cannot be computed with accuracy, but which imply a pulse group more densely populated on the high energy side; this situation frequently obtains. We take the normalized group

$$\frac{k}{1-e^{-k}} e^{k(1-z)} \quad 0 \leq z \leq 1,$$

where  $z$  is the pulse height in terms of the maximum. If the noise spectrum is Gaussian with variance  $\sigma^2$ , the probability of finding a pulse of height greater than  $z$ , is

$$\begin{aligned} B(z) &= \frac{\exp(\frac{1}{2}k^2\sigma^2 - k)}{2(1-e^{-k})} \left\{ e^{kz} \left( \operatorname{erf} \left( \frac{1}{\sqrt{2}\sigma} z + \frac{k\sigma}{\sqrt{2}} \right) - \operatorname{erf} \left( \frac{1}{\sqrt{2}\sigma} (z-1) + \frac{k\sigma}{\sqrt{2}} \right) \right) \right. \\ &\quad \left. + \exp(-\frac{1}{2}k^2\sigma^2 + k) \operatorname{erf} \left( \frac{1}{\sqrt{2}\sigma} (z-1) \right) - \exp(-\frac{1}{2}k^2\sigma^2) \operatorname{erf} \left( \frac{z}{\sqrt{2}\sigma} \right) \right\}, \end{aligned}$$

where

$$\operatorname{erf} x = \frac{2}{(\pi)^{\frac{1}{2}}} \int_x^{\infty} \exp(-t^2) dt.$$

(It is tabulated by Jahnke and Emde.<sup>79</sup>)

Appropriate values for our own work were  $k \sim 10$ ,  $\sigma \sim 0.1$ .

<sup>81</sup> J. O. Hirschfelder and J. L. Magee, *Phys. Rev.* **73**, 207 (1948).